Available online at www.sciencedirect.com
SCIENCE DIRECT
Vision Research 46 (2006) 1282–1291
Vision Research
www.elsevier.com/locate/visres

Shape analysis of female facial attractiveness

Dario Riccardo Valenzano [a], Andrea Mennucci [a], Giandonato Tartarelli [a], Alessandro Cellerino [a,b,*]

[a] Scuola Normale Superiore, Pisa, Italy
[b] Institute of Neuroscience, CNR, via Giuseppe Moruzzi 1, 56100 Pisa, Italy

Received 26 November 2004; received in revised form 14 October 2005

Abstract

Previous studies have suggested that female facial attractiveness is associated with exaggerated sex-specific facial traits and averageness. Here we applied geometric morphometrics, a method for multivariate statistical analysis of shape, to measure geometric averageness and geometric sexual dimorphism of natural female face profiles. Geometric averageness and geometric sexual dimorphism correlate with attractiveness ratings. However, principal component analysis extracted a shape component robustly correlated with attractiveness but independent of sexual dimorphism. The shape differences between attractive- and hyperfeminine traits are localised: attractive facial shape and sexual dimorphism are similar in the upper face, but are markedly distinct in the jaw and chin.

Keywords: Face perception; Geometric morphometrics; Morphing; Evolutionary psychology; Sexual selection

1. Introduction

Facial attractiveness has been investigated extensively in recent years using morphing programmes (Cellerino, 2003; Fink & Penton-Voak, 2002; Grammer, Fink, Moller, & Thornhill, 2003; Little & Perrett, 2002; Rhodes & Zebrowitz, 2002; Thornhill & Gangestad, 1999). Two geometric parameters were correlated to female facial attractiveness: "averageness", i.e., conformity to the population average shape, and "femininity", i.e., conspicuousness of sexually dimorphic traits (Deffenbacher, Vetter, Johanson, & O'Toole, 1998; Grammer & Thornhill, 1994; Langlois & Roggman, 1990; Perrett et al., 1998). The theory of sexual selection lends general explanations for these observations which would create a parallel between a large body of behavioural studies in animals and human perception: preference for average traits can be interpreted as the result of stabilising selection and preference for enhanced femininity as the result of directional selection for extreme sexual traits (Andersson, 1994).

To investigate the geometry associated with attraction, most studies have warped an averaged face along pre-defined directions (typically the male–female direction). The facial stimuli created using this method are close in shape to the average face and do not cover *natural* variation of face shapes. One feasible approach to probe the geometry of natural faces is to represent faces as points in a "face space" where the geometric variation is reduced in complexity and each face is represented by a tractable vector. This approach was first suggested by Valentine (1991). One method to create a face space is principal component analysis (PCA). A face space based on PCA was first proposed for automated face recognition (Turk & Pentland, 1991). A more sophisticated method of PCA separates the texture and shape components (O'Toole, Vetter, Troje, & Bulthoff, 1997). The dimensionality of these spaces is however still large and PCA, which are defined as the eigenvectors of the data covariance matrix, are statistically uncorrelated but are neither strictly independent nor correspond necessarily to an orthonormal (Euclidean) space in geometrical sense (for discussion see Stone, 2002). An approach used to simplify the dimensionality of face space is the reduction of faces to

* Corresponding author. Tel.: +39 050 3153198; fax: +39 050 3153212.
E-mail address: cellerino@in.cnr.it (A. Cellerino).

0042-6989/$ - see front matter © 2005 Elsevier Ltd. All rights reserved.
doi:10.1016/j.visres.2005.10.024

"face cubes" where texture differences are eliminated and faces are defined by only 37 anthropometric distances (Wilson, Loffler, & Wilkinson, 2002). The important result of the "face cube" approach is the demonstration that the perceptual representation of face space is locally Euclidean.

Geometric morphometrics (GM) is a method for multivariate analysis of shape (Bookstein, 1996; Dryden & Mardia, 1998; Rohlf, 1998) which has become the method of choice for analysis of craniofacial shape (Bookstein, 1996; Harvati, 2003; Hennessy, Kinsella, & Waddington, 2002; Mitteroecker, Gunz, Bernhard, Schaefer, & Bookstein, 2004; Ponce de Leon & Zollikofer, 2001; Rosas & Bastir, 2002; Vioarsdottir, O'Higgins, & Stringer, 2002; Zollikofer & Ponce De Leon, 2002). GM shares several features with the previous approaches in that it represents shape variation as vectors in a morphometric space, but it also has some important distinguishing features. GM describes shape as an ordered sets defined the coordinates of *homologous* points named landmarks (Dryden & Mardia, 1998). Landmarks are points whose correspondence can be identified unambiguously in each faces (for example the corners of the eyes, the corners of the mouth, ...) and are the foundation of physical anthropology. The scatter of these points around the consensus shape of the shape set defines a morphometric space. This space supports a distance, the *Procrustes* distance, which is rigorously defined as a shape distance. If applied to face perception, Procrustes distance quantifies the difference *in shape* of a face from the average face and provides a measure for averageness.

In GM, shape differences are represented as deformations of a Cartesian grid where the deformations generated by movements of the landmarks are interpolated by the *thin plate spline* (TPS) function. Beside being a convenient way of graphically representing shape changes, the TPS can be spectrally decomposed in its eigenfunctions. Like the coefficients of the harmonics for Fourier analysis, the coefficients of these eigenfunctions (named partial warps) are an orthonormal (Euclidean) base for face space. The relevant point here, is that each face is represented by its coordinates on the orthogonal set of principal warp axis. In this representations, the axis of sexual dimorphism is simply the axis which connects the average male and female faces.

In summary, GM, by reducing shape variation into the variations in the positions of defined anthropometric landmarks, allows a direct measure of averageness and sexual dimorphism. Therefore, we used GM to assess the effects of averageness and sexual dimorphism on attractiveness of female profiles.

Profiles were analysed for the following reasons:

(i) Geometry is more salient for gender classification in lateral views while gender classification in frontal views is based mostly on texture (Bruce & Langton, 1994; Hill, Bruce, & Akamatsu, 1995).

(ii) Several anthropometric landmarks (glabella, nasion, rhinion, pogonion, ...), which represent the dataset used for GMM, can be located only in lateral views.

(iii) Lateral views avoid the computational problems associated with the analysis of landmarks with bilateral symmetry (Dryden & Mardia, 1998; Klingenberg, Mebus, & Auffray, 2003; Zollikofer & Ponce De Leon, 2002).

Most studies of facial attractiveness have used frontal portraits as stimuli (Rhodes & Zebrowitz, 2002). A strong correlation in the attractiveness of frontal and profile body views is reported (Tovee & Cornelissen, 2001) but, surprisingly, no such study was performed yet on facial views.

We first demonstrated that facial attractiveness in frontal and lateral views is highly correlated. We then followed these steps:

(i) texture variation in natural faces was eliminated using a morphing programme,

(ii) these texture-normalised facial stimuli were rated for attractiveness,

(iii) facial shape was reduced to the position of 21 anthropometric landmarks,

(iv) a morphometric space was created and the distance of each female face form the female average shape was calculated and correlated with her attractiveness rating,

(v) sexual dimorphism was calculated as the projection of individual faces on the male–female axis in morphometric space and correlated with attractiveness ratings,

(iv) multiple regression was used to identify the direction of attractiveness in morphometric space and this direction was compared with the male–female direction.

The result of this analysis is that averageness and sexual dimorphism both correlate with attractiveness ratings but there are components of facial attractiveness independent from sexual dimorphism.

2. Materials and methods

2.1. Models and photographic setting

Thirty-three adult female (age range 17–30) and 33 adult male (age range 17–33) faces were photographed in side-portrait in a professional studio using a digital camera. Twenty-seven out of 33 female subjects were also portrayed in frontal view. Models were photographed at a distance of 3.5 m with a 105 mm teleobjective to minimise distortions. A second person checked that the face of the subject was orthogonal to the optic axis of the objective and the head was not tilted laterally. Heads were all in the "Frankfurt plane", i.e., with the *auriculare* (a craniofacial landmark corresponding to the top of the ear opening) aligned with the orbital basis. Two diffused frontal lights were used to create homogeneous lightning. Several shots were taken for each subject and two of the authors (D.R.V. and A.C.) independently selected the shot which appeared to show the most neutral expression. Pictures were cropped and then reduced to a dimension of 600×800 pixels.

2.2. Morphing

An averaged female face was generated using the same procedure of Perrett et al. (1998) by calculating the average female face shape, unwarping all pictures to conform to this shape and then blending them using GtkMorph. GtkMorph is a morphing programme; it was developed by one of the authors (A.M.); it is freely available on http://xmorph.sf.net.

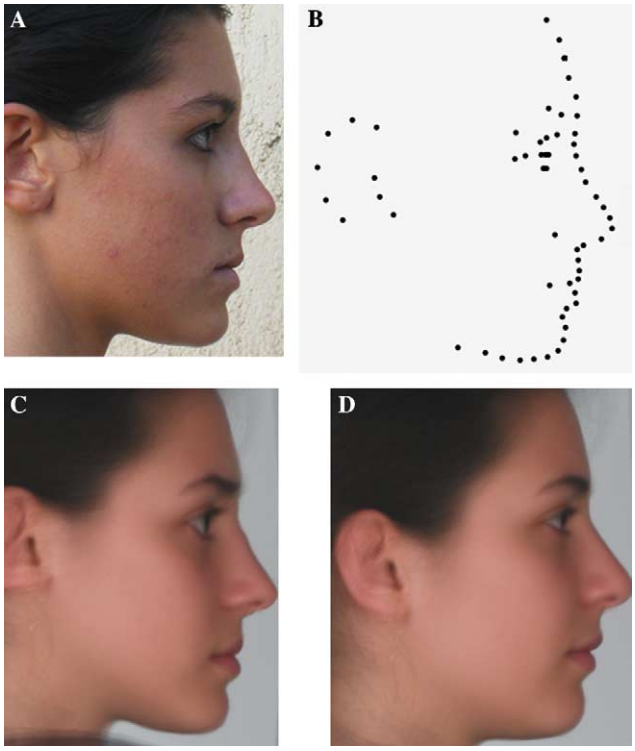

Fig. 1. Face morphing using GTKMorph. (A) A side portrait of one individual face from the sample. (B) Distribution of the landmarks used for morphing of the face in (A). (C) Face (A) overlaid with averaged texture maintaining face shape unmodified. (D) Averaged female face.

Using GtkMorph, we can fix some landmark points on face images; then, GtkMorph creates a smooth mesh that interpolates and extrapolates these points. This mesh is computed minimizing iteratively the "bending energy" (a second-order functional, that is expressed on page 7 in http://xmorph.sf.net/hbes04_pub.pdf). The "bending energy"

$$\min \iint \left\| \frac{\partial^2 f}{\partial x^2} \right\|^2 + 2\left\| \frac{\partial^2 f}{\partial xy} \right\|^2 + \left\| \frac{\partial^2 f}{\partial y^2} \right\|^2 \mathrm{d}x\,\mathrm{d}y$$

is the energy whose closed-form minima was introduced in (Bookstein, 1996) with the name of "thin plate spline function"; the "thin plate spline function" is a fundamental tool in geometric morphometrics.

GtkMorph then can compute a weighted morph of all input images. By morphing, we mean a clever combination of "warping" and "blending": first, all input images are warped into an average shape; second, the warped images are blended. This whole process is explained in pages 2–4 in http://xmorph.sf.net/hbes04_pub.pdf. The warping algorithm used in GtkMorph is an improvement of the original algorithm published in George Wolberg's "Digital Image Warping" (IEEE Computer Society Press order number 1944); it indeed implements an antialiasing Lanczos kernel, that provides higher resolution, as shown in pages 11–13 of http://xmorph.sf.net/hbes04_pub.pdf. To obtain realistic face pictures, faces were annotated by 121 facial points (Figs. 1A and B). A subset of these points is the anthropometric landmarks listed in Table 1, but others needed to be added to obtain faces which had the appearance of natural faces but also conformed to the geometry of the original faces. The use of a smaller number of landmarks did not result in faces which conformed exactly to the geometry of the target face. Each individual morph was inspected by two of the authors (D.R. and A.C.) and the position of the landmarks was adjusted until the quality shown in Fig. 1 was reached for all 33 stimuli.

2.3. Attractiveness rating

Male subjects ($n = 15$, age 19–30) were recruited among Biology University students. To each of the subject, all the faces were presented in randomised order onto a 15 in. computer screen (images were down-sampled at 400×300 pixel, 72 dpi resolution). The subjects were instructed to rate

Table 1
Facial anthropometric landmarks for morphometric analysis

Landmark	Description
1. Superciliare	Highest point of the upper margin of the midline portion of the eyebrow (type I)
2. Frontozygomaticus	Most lateral point of the eyebrow (type I)
3. Exocanthion	Lateral hinge when the eyelid closes (type I)
4. Palperbrale superius	Highest point of the eyelid when the eye is relaxed open (type I)
5. Palperbrale inferius	Lower point of the eyelid when the eye is relaxed open (type I)
6. Glabella	Most lateral point of the forehead (type II)
7. Nasion	Most inner point on the nose ridge within the eye region (type II)
8. Rhinion	Anterior tip at the end of the suture of the nasal bones (type II, estimated by the bridge of the nose)
9. Nose tip	Nose tip (type II)
10. Alare	Most lateral point of the nose (type II)
11. Columella	Most anterior point of the nostril opening (type II)
12. Upper lip	Highest point on the upper lip (Type I)
13. Lower lip	Lowest point on the lower lip (Type I)
14. Stomion	Midline point between upper and lower lip (type I)
15. Cheilion	Most lateral point where the upper and lower lip meet (type I)
16. Subnasale	Most inner point between the nose tip and the upper lip (type II)
17. Chin fissure	Most inner point between pogonion and lower lip (type II)
18. Pogonion	Most anterior point of the chin (type II)
19. Gnation	Lowest point of the chin (type II)
20. Gonion	The maximum curvature point at the angle of the mandible (type II)
21. Auditory canal base	Lowest point on the auditory canal ridge (type I)

the faces on a 7-point Likert's scale (1 = very unattractive, 2 = unattractive, 3 = quite unattractive, 4 = average, 5 = quite attractive, 6 = attractive, 7 = very attractive).

2.4. Landmarks

Geometric morphometrics describe shape as an ordered set of *homologous* points named landmarks (Bookstein, 1996; Dryden & Mardia, 1998). So, comparisons are made only between set of objects where homologous points can be identified. Landmarks are further divided into type I landmark, which corresponds to the point of junction between two histologically different structures (such as bone suture, eye corners, ...), and can be identified with very high precision and type II landmarks defined geometrically (e.g., the gonion, the point of maximum curvature of the jaw) which need careful orientation of the picture to be annotated precisely.

A list of the landmarks we used in our study is given in Table 1. Fig. 2 shows the position of the landmarks on an individual face.

2.5. Geometric morphometrics

2.5.1. Construction of face space

The methodology of GM is described in Bookstein (1997) and Dryden and Mardia (1998). Freely available softwares for GM can be downloaded from http://life.bio.sunysb.edu/morph/. The procedure is briefly described here, for a formal description of GM the readers are referred to Bookstein (1997) and Dryden and Mardia (1998). The basic steps of GM are:

Fig. 2. Set of 21 facial landmarks used in the geometric morphometrics analysis. See Table 1 for definition of landmarks.

1. Shapes are reduced to an ordered set of landmark coordinates.
2. Shapes are scaled to unitary centroid size and rotated for maximum overlap.
3. The consensus shape, in this case the consensus of all male and female faces, is computed. This shape represents the origin of the face space.
4. The axis of the face space (principal warps) is computed and each face is represented as a point in the face space defined by the principal warps axis. Principal warps are an *orthonormal* base for face space which allows to define directions, angles and distances.
5. Principal warps (which *are not* principal components) can be used as the input of a principal component analysis if further compression of the space dimensionality is necessary.

2.5.2. Geometric sexual dimorphism and angles in face shape

A measure of geometric sexual dimorphism can be easily derived in face shape by calculating the coordinates of the consensus male and consensus female shapes. The axis which connects these two shapes strictly defines the axis of sexual dimorphism. The geometric sexual dimorphism of individual faces is defined as the position along this axis (Fig. 3A). If $\vec{F}_i$ is the vector in face space corresponding to an individual face, geometric sexual dimorphism (GSD) is the norm of the orthogonal projection of this vector on the male–female axis divided by the norm of vector corresponding to the average female face $\vec{F}_{avg}$

$$\mathrm{GSD} = \frac{\langle \vec{F}_i \cdot \vec{F}_{avg} \rangle}{\|\vec{F}_{avg}\|^2} = \frac{\|\vec{F}_i\|}{\|\vec{F}_{avg}\|} \cos\theta. \quad (1)$$

This scalar quantity equals -1 for the average male face and 1 for the average female face. If GSD <-1 the face is hypermasculine and if GSD >1 the face is hyperfeminine.

This formula allows us to measure also the angle θ between the two vectors in face shape as

$$\theta = \arccos\left(\frac{\langle \vec{F}_i \cdot \vec{F}_{avg} \rangle}{\|\vec{F}_{avg}\|^2}\right). \quad (2)$$

2.5.3. Attractive mean shape and test for differences of directions in face space

The 33 female faces were divided into seven discrete classes, each containing five faces with the last containing only three faces, in ascending order of rated attractiveness. So the five faces with the lowest attractiveness

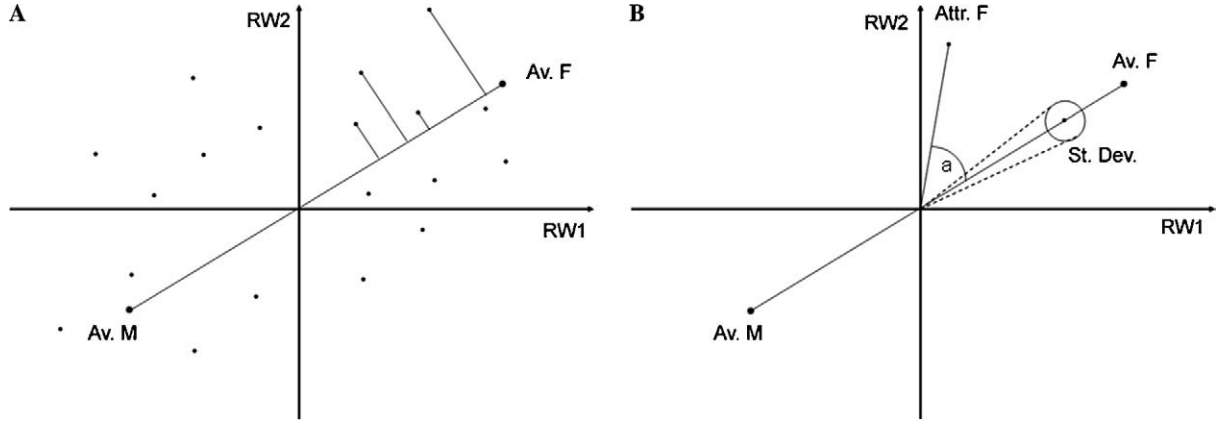

Fig. 3. Schematic representation of the "face space". Each face shape is represented as a point in an N-dimensional space. Only two axes are represented for ease of illustration. (A) Geometric sexual dimorphism. Av.M and Av.F identify the position of the consensus male and female shape. The axis connecting Av.M and Av.F is the axis of sexual dimorphism. Geometric sexual dimorphism (GSD) is the norm of the orthogonal projection of each individual face vector on the male–female axis divided by the norm of vector corresponding to the average female face. (B) Bi-dimensional representation of independence between attraction weighted face shape (Attr. F) and average female face (Av. F). The two points have the same distance from the origin, *a* is the angle formed by these two vectors in the face shape space. The dotted circle identifies the hypersphere with radius equal to the standard deviation of the averaged female shape.

were assigned a weight of 1, the second five faces a weight of 2, and so on. We then computed the weighted consensus shape. The distance of this shape from the origin of face space (that is the average of all male and female faces) was adjusted to be the same as the geometrically averaged female shape. We called this new average face perceptually weighted mean shape (PWM).

The angle between the PWM and the average female shape was computed using formula (2). To assess the confidence in the computation of this angle, a second angle was computed based on the vector $\vec{C}$, which has as coordinates the 95% confidence intervals for each principal warp coordinate of the average females shape (Fig. 3B). The confidence interval of the angle φ can be easily computed as

$$\varphi = \arctan\left(\frac{\|\vec{C}\|}{\|\vec{F}_{\text{avg}}\|}\right). \quad (3)$$

2.5.4. Multiple regression

As an independent measure of the direction in face space associated with attractiveness, we estimated its vector by a multiple regression. A principal component analysis (PCA) of shape was performed (Dryden & Mardia, 1998). Basically, the principal warp coordinates of all 66 faces were used as input for a conventional PCA, this approach further reduces the dimensionality of the face space: the first 15 PC account for more than 98% of face shape variation.

Similar to what described in formula (1), the grand average represents the origin of PC space and the average female face is a vector defined by its PC coordinates

$$\vec{F}_{\text{avg}} = (pc_1^f, pc_2^f, \ldots, pc_{15}^f).$$

A multiple regression analysis of the PCA scores against attractiveness ratings identifies a vector defined by the β coefficients of the linear regression. The vector

$$\vec{\beta} = (\beta_1, \beta_2, \ldots, \beta_{15})$$

is the vector orthogonal to the regression hyperplane, i.e. orthogonal to the direction of attractiveness in morphometric space. The angle between $\vec{F}_{\text{avg}}$ and $\vec{\beta}$ can be measured using Eq. (2).

2.6. Statistics

Statistical analysis was performed using STATISTICA 5.1® (StatSoft Inc., 1997). Two-tailed Pearson's r coefficient was used to test for correlation at the .05 level. Multiple regression was performed using PCA scores as independent variables and attractiveness ratings as the dependent variable. Cronbach's α was used as index of inter-rater reliability.

3. Results

3.1. Face shape statistics

GM requires manual annotation of well-defined anthropometric landmarks. To estimate the systematic error in manual annotation, three female and three male faces were annotated five times each. The maximum Procrustes distance (the shape distance of morphometric space (Dryden & Mardia, 1998) between each pair of the different annotations of the same was then compared with the distribution of Procrustes distances between individual faces of each sex and the consensus shape of the corresponding sex. The systematic error in landmark annotation was 0.3% of the median Procrustes distance within each sex.

Fig. 4A reports the scatter of the 33 male and 33 female faces superimposed to the grand (male + female) average after Procrustes superposition. Fig. 4B illustrates the consensus male and female faces. Shape dimorphisms can be better appreciated in Figs. 4C and D, where differences from the androgynous (grand average) shape are visualised as a Cartesian deformation grids (thin plate splines (Dryden & Mardia, 1998)). Regions of maximum grid strain localise regions of maximum sexual dimorphism and the thin plate splines corresponding to the consensus male and female faces. X2 extrapolation of shape differences was applied for better visualisation. Fig. 4E reports the distribution of the Procrustes distances of the individual males from the male consensus and the individual female faces from the female consensus. The mean Procrustes distance does not differ between the sexes (Mann–Whitney U test, $p > 0.3$). Geometric sexual dimorphism (GSD) for each face shape was measured as the coordinate on the male–female axis (see Section 2 for details). The values of GSD for the two sexes are reported in Fig. 4F. It is evident from Fig. 4F that GSD clearly separates male and female faces (correct classification 90%) demonstrating that the limited number of landmarks used in this study is sufficient to capture shape dimorphism.

3.2. Attractiveness of face profiles

Most studies of facial attractiveness used frontal portraits as stimuli (Rhodes & Zebrowitz, 2002). A strong correlation in the attractiveness of frontal and profile body views is reported (Tovee & Cornelissen, 2001) but similar data for facial pictures are missing.

We had 27 female frontal pictures rated for attractiveness by 15 young men (age 22–35) and the profile pictures of the same females rated by a different sample of 15 young men (age 23–31). A very high correlation between the frontal and lateral ratings was observed (Pearson's $r = 0.6558$, $p < 0.0001$).

To eliminate the effects of texture on attractiveness, an averaged female profile was created by morphing (Fig. 1D). Using a well-established procedure (Fink, Grammer, & Thornhill, 2001; Little & Hancock, 2002; Perrett et al., 1998), the averaged female colour map was warped to fit the geometry of 33 individual female faces (Figs. 1A and C) creating stimuli of uniform texture. The 33 faces were rated by 20 male subjects (age 22–30). In line with previous results (Rhodes & Zebrowitz, 2002), high inter-rater reliability for attractiveness ratings was recorded (Cronbach's $\alpha = 0.92$).

A perceptually averaged female shape (Fig. 5A) was created by using attractiveness ratings as weights in the shape averaging (see Section 2) this "attractive" shape has the same Procrustes distance from the androgynous shape than the consensus female shape but identifies the vector of maximum increase in attractiveness when moving away from the androgynous shape. We have then confronted the attractiveness direction with the direction of sexual dimorphism.

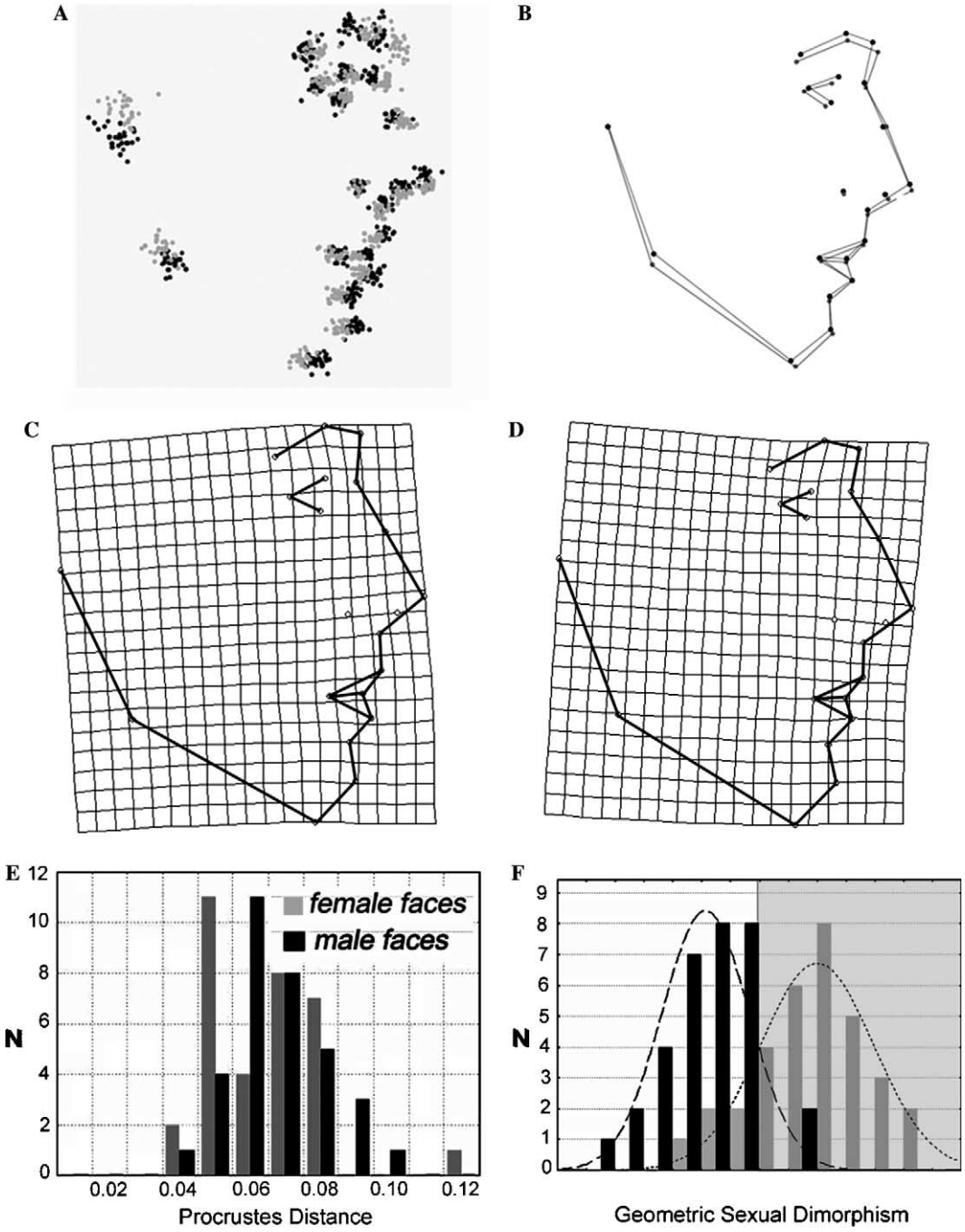

Fig. 4. Face space statistic. (A) Aligned scatter of the face landmarks for 33 female faces (black points) and 33 male faces (grey points) annotated by the 21 morphometric landmarks. (B) Consensus female (black) and male (grey) face shape. (C and D) Thin plate spline representation of the shape changes by transformation of the grand average-face shape consensus into the female-face shape consensus (C) or the male-face shape consensus (D). (E) Distribution of Procrustes distances of individual faces from the consensus of their gender. Grey bars, female faces; black bars, male faces. (F) Distribution of geometric sexual dimorphism measured as schematised in Fig. 3. Grey bars, female faces; black bars, male faces.

Fig. 5B illustrates the hyperfeminine shape obtained by extrapolating the differences between the consensus androgynous- and female shapes. Attractive- and hyperfeminine shapes are not coincident. This difference is better appreciated in Fig. 5C where the attractive shape was subtracted from the hyperfeminine shape. This subtraction highlights the differences between attractiveness and sexual dimorphism. These are more visible (the thin plate spline is more bent) in the jaw and chin: with respect to the hyperfeminine shape, the attractive shape has a smaller, but more pointed, chin, more angled jaw, less prominent alveolar prognathism.

To demonstrate that the attractiveness and dimorphism are different trajectories in shape space, we calculated the angle between the male–female axis and the attractiveness

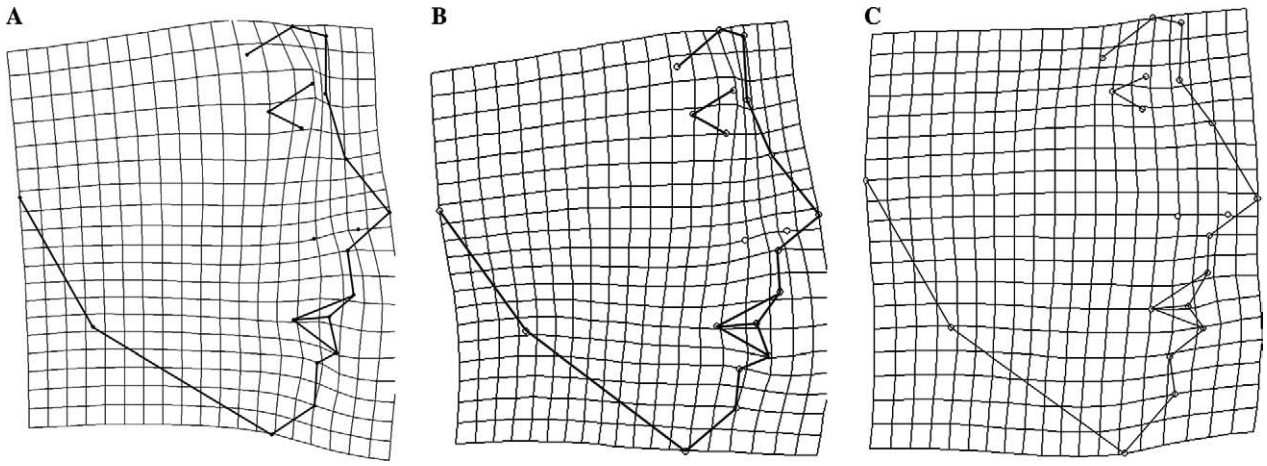

Fig. 5. (A) Perceptually averaged female face, obtained using attractiveness scores as weights in the averaging process and expressed as a thin plate spline deformation grid enhanced by a factor 5. (B) Hyperfeminine female face, obtained by morphing the average female face 50% away from the grand average (androgynous) face and expressed as a thin plate spline deformation grid enhanced by a factor 5. (C) Thin plate spline visualisation of shape difference between (B) and (A), i.e., (C) must be summed to (A) for obtaining (B).

axis in morphometric space by: (a) computing the angle between the attractive shape and the female average shape and (b) computing the angle between the male–female axis and the hyperplane of multiple regression which provides the best fit of attractiveness scores (see Section 2). These angles are 49° and 56°, respectively. To test for the significance of these angles, we compared them with the angle of the vector defined by the standard deviation of the averaged females shape (see Section 2). This angle is 6° (Fig. 3B).

We tested the effect of averageness on attractiveness by using Procrustes distance, the shape distance of morphometric space (Dryden & Mardia, 1998). The higher the Procrustes distance of an individual shape from the consensus shape, the less average a shape. A significant negative correlation between Procrustes distance and attractiveness ratings was detected ($r = -0.35$, $p = 0.047$, Fig. 6A).

We then calculated the correlation between the geometric sexual dimorphism and attractiveness. A positive correlation was detected (Fig. 6B, $r = 0.34$, $p = 0.05$). These correlations may be judged small by the standards of visual psychophysics, yet it should be considered that the behavioural measure here is not that of a simple percept, but an explicit rating of a psychological perception.

Finally, we performed a principal component analysis of shape (Dryden & Mardia, 1998) and analysed the first 18 PC axis, which accounts for more than 95% of shape variance. As a first analysis, we tested which of the PC axis was correlated with face sex or GM. It is expected that the male–female difference is the principal source of shape variance and, according to predictions, there is a significant difference between the male and female PC1 scores (Mann–Whitney U test $p < 0.001$). PC1 is also strongly correlated with GM ($r = -0.61$, $p < 0.001$). A second PC strongly correlated with face sex is PC5. PC5 scores are statistically different in the two sexes (Mann–Whitney U test $p < 0.001$) and PC5 is correlated with GM ($r = -0.42$, $p = 0.001$). A linear combination of PC1 and PC2 supports 83% correct sex classification in a discriminant analysis (Wilks'-$\lambda = 0.61$, $p < 10^{-6}$). However, neither PC1 nor PC5 correlates with attractiveness ratings ($r = -0.23$ and $r = -0.14$, respectively). We then tested the correlation for each of the PC axis with attractiveness ratings (see Section 2). Statistically significant correlation was detected one PC axis only, PC9 (Fig. 6C, $r = 0.63$, $p < 0.001$). Distribution of PC9 in the two sexes, however, overlaps to a large degree (Fig. 6D), and PC9 does not correlate with GM ($r = 0.18$, $p = 0.15$). PC9, therefore, captures attractiveness but not sexual dimorphism.

To further demonstrate that PC9 captures a component of attractiveness, we randomly extracted nine faces form our face sample set and for each of the faces we produced a pair of pictures: one where PC9 was subtracted and one where PC9 was added. As a control, we produced three more pairs by adding and subtracting PC2, 10 and 18 to the averaged face. All these faces were presented in a forced choice paradigm to 30 male subjects (age 18–32). For six out of the nine faces, a clear preference (>70%) for the PC9+ component of the pair was detected (Fig. 7). A composite χ^2 test on all nine pairs demonstrated a statistically significant preference of the PC9+ face ($p = 0.04$). On the other hand, no bias was detected for PC2, PC10 and PC18 (χ^2, $p = 0.8$).

4. Discussion

In the present study, we used geometric morphometrics (Dryden & Mardia, 1998) to analyse the correlation between shape statistics and attractiveness in a set of natural profiles. GM reduces shape variation to variation in the coordinates of defined anatomical landmarks. Geometric sexual dimorphism measured by GM is an excellent diagnostic indicator of face sex, indicating that the landmarks capture the relevant components of sex-associated facial shape variation. We found correlation of averageness and

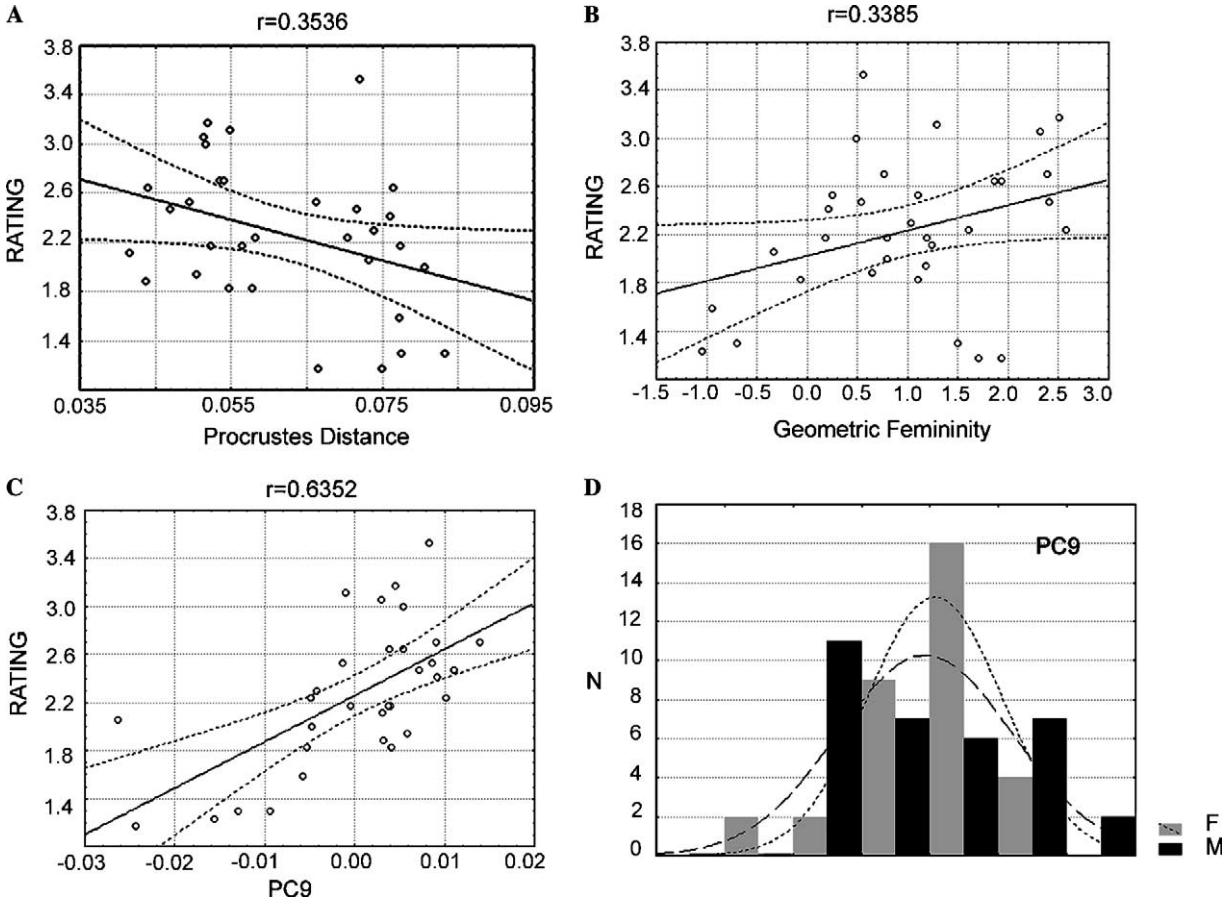

Fig. 6. (A) Correlation between Procrustes distance and attractiveness ratings in the female sample. (B) Correlation between geometric sexual dimorphism and attractiveness in the female sample. (C) Correlation between coordinate on the PC9 axis and attractiveness in the female sample. (D) Distribution of PC9 scores in the female face sample.

sexual dimorphism with attractiveness as suggested by several previous studies (Deffenbacher et al., 1998; Grammer & Thornhill, 1994; Johnston, Hagel, Franklin, Fink, & Grammer, 2001; Langlois & Roggman, 1990; Perrett et al., 1998; Rhodes, Hickford, & Jeffery, 2000; Rhodes et al., 2001). Preference for exaggerated sexual traits is predicted by sexual selection theory and is observed in animal studies (Andersson, 1994) and is also consistent with simple models of perceptual learning (Ghirlanda, Jansson, & Enqvist, 2002). It was suggested that sexually selected traits are indicators of phenotypic quality and individuals with conspicuous sexual traits have higher heritable fitness (good genes hypothesis, see Andersson, 1994). Facial sexual dimorphism is the result of morphogenic action of sexual hormones during infancy and puberty, and it was suggested that attractive facial traits signal for hormonal competence and, in females, fertility (Dryden & Mardia, 1998; Johnston & Franklin, 1993; Johnston et al., 2001). Our study, however, reveals that attractiveness and sexual dimorphism correspond to partially different directions in morphometric space. In the upper face, the shape changes associated with attractiveness are similar, but in the jaw the differences between attractive- and hyperfeminine shape components are strikingly distinct. Sexual dimorphism in female direction is associated with horizontal reduction of the chin, forward movement of the gonion (jaw angle) and alveolar prognathism. On the other hand, attractive shapes are associated with a small, but pointed, chin and do not show exaggerated alveolar prognathism or reduction of gonion angle. Similar attractive shape patterns of the chin were described previously using composite images and morphing techniques (Johnston & Franklin, 1993; Perrett et al., 1998) but were interpreted as hormonal signals (Johnston & Franklin, 1993). The use of GM, however, demonstrates that an important contribution to female attractiveness is given by shape component that is not sexually dimorphic and is localised mainly to the jaw and lower face. Interestingly, the jaw is the region of the human cranium with the longest development (Vioarsdottir et al., 2002) and is strongly influenced by facial growth (Rosas & Bastir, 2002). So attractiveness might be correlated with biological phenomena that are operative during early adulthood. Our study confirms a contribution of sexual dimorphism to female facial attractiveness, but also highlights that attractiveness is not coincident with exaggeration of sexual dimorphism, but is associated with a specific pattern of shape variation, particularly in the jaw. The biological meaning of this pattern remains to be investigated.

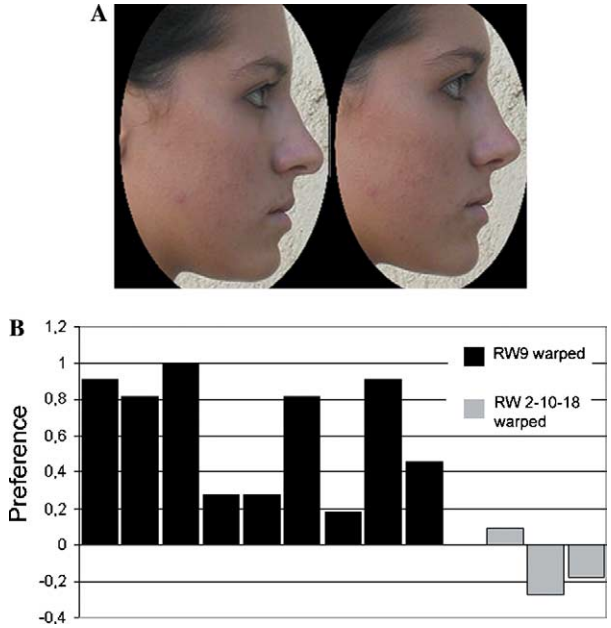

Fig. 7. Effects of PC9 on attraction of real faces. (A) Individual face from the sample is morphed along the PC9 axis (−20% left, +20% right). This same transformation was performed on a total of nine faces from the sample. As a control, the averaged face was morphed along PC2, 10 and 18. (B) Scores of the forced choice test. Represented is the preference bias in the forced choice experiment: the 0 value on the *Y* axis indicates even distribution of preferences (50% for −PC9, 50% for +PC9) and 1 indicates 100% of preference for the +PC9. The nine black bars correspond to the nine individual faces. In grey are represented the preferences for the transformations along PC2, 10 and 18. (Total number of subjects tested = 30.)

Acknowledgments

This work was supported by Scuola Normale Superiore SNS-03 grant and the MIUR Grant No. 2003062952.

References

Andersson, M. (1994). *Sexual selection. Monographs in behaviour and ecology*. Princeton, NJ: Princeton University Press.

Bookstein, F. L. (1996). Biometrics, biomathematics and the morphometric synthesis. *Bulletin of Mathematical Biology, 58*(2), 313–365.

Bookstein, F. L. (1997). *Morphometric tools for landmark data geometry and biology*. (pp. xvii, 433 s.). Cambridge: Cambridge University Press.

Bruce, V., & Langton, S. (1994). The use of pigmentation and shading information in recognising the sex and identities of faces. *Perception, 23*(7), 803–822.

Cellerino, A. (2003). Psychobiology of facial attractiveness. *Journal of Endocrinological Investigation, 26*(3 Suppl.), 45–48.

Deffenbacher, K. A., Vetter, T., Johanson, J., & O'Toole, A. J. (1998). Facial aging, attractiveness, and distinctiveness. *Perception, 27*(10), 1233–1243.

Dryden, I. L., & Mardia, K. V. (1998). *Statistical shape analysis*. Chichester: Wiley, p. 347 s.

Fink, B., Grammer, K., & Thornhill, R. (2001). Human (*Homo sapiens*) facial attractiveness in relation to skin texture and color. *Journal of Comparative Psychology, 115*(1), 92–99.

Fink, B., & Penton-Voak, I. (2002). Evolutionary psychology of facial attractiveness. *Current Directions in Psychological Science, 11*(5), 154–158.

Ghirlanda, S., Jansson, L., & Enqvist, M. (2002). Chicken prefer beautiful humans. *Human Nature, 13*, 383–389.

Grammer, K., Fink, B., Moller, A. P., & Thornhill, R. (2003). Darwinian aesthetics: Sexual selection and the biology of beauty. *Biological Review of the Cambridge Philosophical Society, 78*(3), 385–407.

Grammer, K., & Thornhill, R. (1994). Human (*Homo sapiens*) facial attractiveness and sexual selection: The role of symmetry and averageness. *Journal of Comparative Psychology, 108*(3), 233–242.

Harvati, K. (2003). The Neanderthal taxonomic position: Models of intra- and inter-specific craniofacial variation. *Journal of Human Evolution, 44*(1), 107–132.

Hennessy, R. J., Kinsella, A., & Waddington, J. L. (2002). 3D laser surface scanning and geometric morphometric analysis of craniofacial shape as an index of cerebro-craniofacial morphogenesis: Initial application to sexual dimorphism. *Biological Psychiatry, 51*(6), 507–514.

Hill, H., Bruce, V., & Akamatsu, S. (1995). Perceiving the sex and race of faces: The role of shape and colour. *Proceedings of the Royal Society of London B Biological Sciences, 261*(1362), 367–373.

Johnston, V. S., & Franklin, M. (1993). Is beauty in the eye of the beholder? *Ethology and Sociobiology, 14*, 183–189.

Johnston, V. S., Hagel, R., Franklin, M., Fink, B., & Grammer, K. (2001). Male facial attractiveness—Evidence for hormone-mediated adaptive design. *Evolution and Human Behavior, 22*(4), 251–267.

Klingenberg, C. P., Mebus, K., & Auffray, J. C. (2003). Developmental integration in a complex morphological structure: How distinct are the modules in the mouse mandible? *Evolution & Development, 5*(5), 522–531.

Langlois, J. H., & Roggman, L. A. (1990). Attractive faces are only average. *Psychological Science, 1*, 115–121.

Little, A. C., & Hancock, P. J. (2002). The role of masculinity and distinctiveness in judgments of human male facial attractiveness. *British Journal of Psychology, 93*(Pt. 4), 451–464.

Little, A. C., & Perrett, D. I. (2002). Putting beauty back in the eye of the beholder. *Psychologist, 15*(1), 28–32.

Mitteroecker, P., Gunz, P., Bernhard, M., Schaefer, K., & Bookstein, F. L. (2004). Comparison of cranial ontogenetic trajectories among great apes and humans. *Journal of Human Evolution, 46*(6), 679–697.

O'Toole, A. J., Vetter, T., Troje, N. F., & Bulthoff, H. H. (1997). Sex classification is better with three-dimensional head structure than with image intensity information. *Perception, 26*(1), 75–84.

Perrett, D. I., Lee, K. J., Penton-Voak, I., Rowland, D., Yoshikawa, S., Burt, D. M., et al. (1998). Effects of sexual dimorphism on facial attractiveness. *Nature, 394*(6696), 884–887.

Ponce de Leon, M. S., & Zollikofer, C. P. (2001). Neanderthal cranial ontogeny and its implications for late hominid diversity. *Nature, 412*(6846), 534–538.

Rhodes, G., Hickford, C., & Jeffery, L. (2000). Sex-typicality and attractiveness: Are supermale and superfemale faces super-attractive? *British Journal of Psychology, 91*(Pt. 1), 125–140.

Rhodes, G., Yoshikawa, S., Clark, A., Lee, K., McKay, R., & Akamatsu, S. (2001). Attractiveness of facial averageness and symmetry in non-western cultures: In search of biologically based standards of beauty. *Perception, 30*(5), 611–625.

Rhodes, G., & Zebrowitz, L. A. (Eds.). (2002). *Facial attractiveness: Evolutionary, cognitive and social perspectives*. Westport, CT: Greenwood Publishing.

Rohlf, F. J. (1998). On applications of geometric morphometrics to studies of ontogeny and phylogeny. *Systematic Biology, 47*(1), 147–158, discussion 159–167.

Rosas, A., & Bastir, M. (2002). Thin-plate spline analysis of allometry and sexual dimorphism in the human craniofacial complex. *American Journal of Physical Anthropology, 117*(3), 236–245.

Stone, J. V. (2002). Independent component analysis: An introduction. *Trends in Cognitive Sciences, 6*(2), 59–64.

Thornhill, R., & Gangestad, S. W. (1999). Facial attractiveness. *Trends in Cognitive Sciences, 3*(12), 452–460.

Tovee, M. J., & Cornelissen, P. L. (2001). Female and male perceptions of female physical attractiveness in front-view and profile. *British Journal of Psychology, 92*(Pt. 2), 391–402.

Turk, M. A., & Pentland, A. P. (1991). Eigenfaces for recognition. *Journal of Cognitive Neuroscience, 3*(1), 71–96.

Valentine, T. (1991). A unified account of the effects of distinctiveness, inversion, and race in face recognition. *Quarterly Journal of Experimental Psychology A, 43*(2), 161–204.

Vioarsdottir, U. S., O'Higgins, P., & Stringer, C. (2002). A geometric morphometric study of regional differences in the ontogeny of the modern human facial skeleton. *Journal of Anatomy, 201*(3), 211–229.

Wilson, H. R., Loffler, G., & Wilkinson, F. (2002). Synthetic faces, face cubes, and the geometry of face space. *Vision Research, 42*(27), 2909–2923.

Zollikofer, C. P., & Ponce De Leon, M. S. (2002). Visualizing patterns of craniofacial shape variation in *Homo sapiens*. *Proceedings of the Royal Society of London B Biological Sciences, 269*(1493), 801–807.